Akademia Baru Publishing (M) Sdn Bhd

Journal of Advanced Research in Numerical Heat Transfer

Journal homepage: www.akademiabaru.com/arnht.html
ISSN: 2735-0142

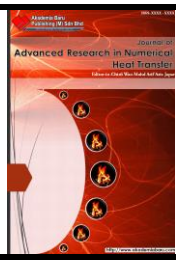

Hydrothermal performance in the Hydrodynamic Entrance Region of Rectangular Microchannel Heat Sink

Open Access

Wan Mohd. Arif Aziz Japar[1,*], Nor Azwadi Che Sidik[1], Natrah Kamaruzaman[2], Yutaka Asako[1], Nura Mu'az Muhammad[3]

[1] Malaysian-Japan International Institute of Technology, Universiti Teknologi Malaysia, 54100 Kuala Lumpur, Wilayah Persekutuan Kuala Lumpur, Malaysia
[2] Department of Thermofluid, School of Mechanical Engineering, Faculty of Engineering, Universiti Teknologi Malaysia, 81310 Skudai, Johor, Malaysia
[3] Faculty of Engineering, Kano University of Science and Technology, Wudil, Nigeria

ARTICLE INFO

Article history:
Received 23 April 2020
Received in revised form 15 June 2020
Accepted 22 June 2020
Available online 30 June 2020

ABSTRACT

Microchannel heat sink is an advanced cooling technique that can fulfil cooling demand for the compact electronic devices which have high power density in its microchip. However, fast development in electronic industry increases the power density rapidly. As consequence, innovation of microchannel heat sink design is required in order to remove the high heat flux generated by the electronic device. In the microchannel innovation, basic problem that has been experienced by the conventional microchannel heat sink (rectangular microchannel heat sink, CR MCHS) need to be identified first before the new microchannel design is proposed. The hydrodynamic entrance region is one of the issues in a microchannel heat sink because it will affect hydrothermal performance in the conventional microchannel heat sink. Thus, in this paper, the effect of hydrodynamic entrance region on fluid flow and heat transfer characteristic had been investigated numerically for the Reynold number of 100 – 800 at the constant wall heat flux of 100 W/cm^2. The result showed that the thermal resistance in the hydrodynamic entrance region of CR MCHS is lower than in the developed region. However, pressure drop in the developing region is higher that developed region due to the highest wall shear stress in the entrance region. For hydrodynamic diameter, Dh = 133 µm, the hydrodynamic entrance length of Re = 100 is 4 mm from channel inlet, while Re = 800 is 9 mm from the channel inlet.

Keywords:
Rectangular microchannel heat sink; hydrodynamic entrance; hydrothermal performance

1. Introduction

Over the past decade, the investigation of fluid flow and heat transfer characteristic induced by natural convection on thermal performance becomes a most interesting topic in a cooling system. The effectiveness of the cooling system in such application is very important to keep the temperature of a structure or electronic device from exceeding limits imposed by needs of safety and efficiency.

* *Corresponding author.*
E-mail address: arifklang@gmail.com (Wan Mohd. Arif Aziz Japar)

The applications of the cooling system in thermal engineering are known for years and have been studied critically in theoretical as well practical point of view in various engineering applications such as building energy system, electronic device, chemical vapor deposition instruments, solar energy collector, furnace engineering and many more [1]. In recent years, rapid growth in the electronic industry has witnessed a new generation high performing dense chip packages in many modern electronic devices. The chip packages that work at high frequency has produced very high heat flux on the electronic devices. If it happens continually, the heat flux will create the hot spot on the electronic device and thus reduces the lifespan of the electronic devices due to the acceleration of the Mean Time to Failure (MTTF) as described by Black's equation [2]. The increase in power density and miniaturization of electronic packages has driven the direction of cooling system technology from the air-cooling technology to the advanced heat transfer technology due to the conventional method inadequate to remove very high heat flux [3]. However, the development of more compact electronic devices that will operate at high power density causes the thermal management of electronic devices becomes a very critical issue in the electronics industry due to lack of efficient technique to remove heat from the devices [4, 5].

During the past 30 years, many methods have been proposed in open literature in order to improve overall performance of microchannel heatsink with minimal thermal resistance and pressure drop that can satisfy the cooling demand. Generally, the methods can be categorized into two groups, active method and passive method. Active method will use external energy in its system while passive method no need for that. Most of researcher has widely used the passive method [6-10] due to its low cost and absence of moving part compared to active method [11-15].

Before a novel microchannel heat sink with complex structure is proposed, the understanding of the basic problem that has been experienced by the conventional design such as rectangular microchannel heat sink (CR MCHS) need to be identified first so that we can find the optimum hydrothermal performance for the proposed microchannel heat sink. The hydrodynamic entrance length is one of the issues in the CR MCHS because it will affect the hydrothermal performance. So, in this paper, the effect of the hydrodynamic entrance length on fluid flow and heat transfer characteristic is studied numerically for Re number of 100 to 800.

2. Geometry Parameter of the Rectangular Microchannel Heat Sink

This rectangular microchannel heat sink (CR MCHS) is made by copper and consist of ten microchannels. However, in order to save the computational cost, only one symmetrical part of the microchannel heat sink is adopted in present simulation as shown in Figure 1(a). Table 1 shows the parameter values for the geometry that illustrated in Figure 1(b).

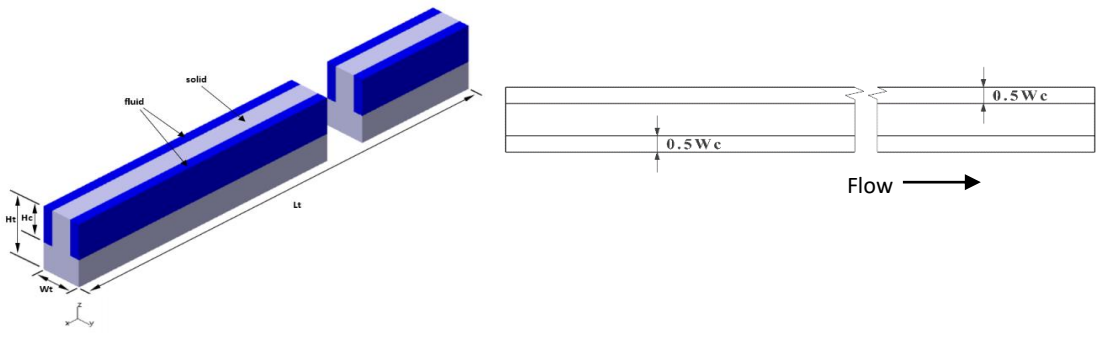

(a) (b)

Fig. 1. CR MCHS (a) One symmetrical part (b) Geometry parameter

Table 1
Geometry parameters of CR MCHS

Lt (μm)	Wt (μm)	Ht (μm)	Hc (μm)	Wc (μm)
10000	200	350	200	100

3. Numerical Method Approach

In order to analyse the hydrothermal performance of CR MCHS, a Computational Fluid Dynamic (CFD) software such as ANSYS FLUENT 17.0 is used to solve the three dimensional fluid flow and heat transfer equations by assuming fluid flow in all simulated designs are continuum due to Knudsen number, (*Kn*) for the fluid flow is less than (10^{-3}) [16]. So, Navier-Stokes equation and non-slip boundary condition are applicable. Besides that, the fluid is assuming as Newtonian, incompressible and has a constant thermophysical properties. The laminar fluid flow and heat transfer are simulated in steady-state. Viscous dissipation, gravitational force and radiation heat transfer are neglected.

3.1 Governing Equations

Based on the assumptions that made in the present study, governing equation for conservation of mass, momentum and energy equations can be written as Eq. (1), Eqs. (2) – (4) and Eqs. (5) – (6), respectively.

$$\frac{\partial u}{\partial x}+\frac{\partial v}{\partial y}+\frac{\partial w}{\partial z}=0 \tag{1}$$

Where *u, v* and *w* are the velocity components in *x*, *y* and *z*-directions respectively. Momentum equation is written as:

$$u\frac{\partial u}{\partial x}+v\frac{\partial u}{\partial y}+w\frac{\partial u}{\partial z}=-\frac{1}{\rho_f}\frac{\partial p}{\partial x}+\frac{\mu_f}{\rho_f}\left(\frac{\partial^2 u}{\partial x^2}+\frac{\partial^2 u}{\partial y^2}+\frac{\partial^2 u}{\partial z^2}\right) \tag{2}$$

$$u\frac{\partial v}{\partial x}+v\frac{\partial v}{\partial y}+w\frac{\partial v}{\partial z}=-\frac{1}{\rho_f}\frac{\partial p}{\partial y}+\frac{\mu_f}{\rho_f}\left(\frac{\partial^2 v}{\partial x^2}+\frac{\partial^2 v}{\partial y^2}+\frac{\partial^2 v}{\partial z^2}\right) \tag{3}$$

$$u\frac{\partial w}{\partial x}+v\frac{\partial w}{\partial y}+w\frac{\partial w}{\partial z}=-\frac{1}{\rho_f}\frac{\partial p}{\partial z}+\frac{\mu_f}{\rho_f}\left(\frac{\partial^2 w}{\partial x^2}+\frac{\partial^2 w}{\partial y^2}+\frac{\partial^2 w}{\partial z^2}\right) \tag{4}$$

Where ρ_f and μ_f are the density and dynamic viscosity of the working fluid, respectively, and *p* is the fluid pressure. There have two energy equations that related to the present study such as energy equation for fluid region, Eq. (5) and energy equation for solid region, Eqs (6):

$$u\frac{\partial T_f}{\partial x}+v\frac{\partial T_f}{\partial y}+w\frac{\partial T_f}{\partial z}=\frac{k_f}{\rho_f c_{Pf}}\left(\frac{\partial^2 T_f}{\partial x^2}+\frac{\partial^2 T_f}{\partial y^2}+\frac{\partial^2 T_f}{\partial z^2}\right) \tag{5}$$

$$0=k_s\left(\frac{\partial^2 T_s}{\partial x^2}+\frac{\partial^2 T_s}{\partial y^2}+\frac{\partial^2 T_s}{\partial z^2}\right) \tag{6}$$

Where T_f, T_s, k_f, k_s and Cp_f are the fluid's temperature, solid's temperature, fluid thermal conductivity, solid thermal conductivity and fluid specific heat, respectively.

3.2 Boundary Condition

Boundary condition is a condition for hydrodynamic and thermal that we applied on the simulated geometries in the present study. Table 2 shows the details for the boundary conditions.

Table 2
Boundary condition for simulation analysis

Boundary	Location	Condition
Hydrodynamic	At the fluid-solid interface	No-slip and no penetration $u=v=w=0$ $-k_s(\frac{\partial T_s}{\partial n})=-k_f(\frac{\partial T_f}{\partial n})$ where n is the coordinate normal to the wall
	At inlet, $x=0$	$u_f=u_{in}$ $v=w=0$
	At outlet, $x=L_t=10mm$	$p_f=p_{out}=1\ atm$
Thermal	At inlet, $x=0$	$T_f=T_{in}=300K$ (for water) $-k_s(\frac{\partial T_s}{\partial x})=0$ (for solid)
	At outlet, $x=L_t=10mm$	$-k_f(\frac{\partial T_f}{\partial x})=0$ (for water) $-k_s(\frac{\partial T_s}{\partial x})=0$ (for solid)
	At the top wall, $z=Ht=0.35mm$	$u=v=w=0$ $-k_s(\frac{\partial T_s}{\partial z})=0$
	At the bottom wall, $z=0$	$-k_s(\frac{\partial T_s}{\partial z})=q_w=100W/cm^2$
	At the sidewall, $y=0$	$\frac{\partial}{\partial y}=0$ (symmetry)
	At the sidewall, $y=Wt=0.2mm$	$\frac{\partial}{\partial y}=0$ (symmetry)

3.3 Grid Independence and CFD Simulation

Mesh quality and number of grid are very important element that will contribute to the convergence of numerical solution and numerical computation stability. In this paper, ANSYS ICEM is used to generate hexahedral meshing structure due to faster solution time with better accuracy than tetrahedral meshing structure. Figure 2 illustrates the hexahedral mesh structure in CR MCHS. Finite volume method is utilized to discretize the governing equation. The SIMPLE algorithm was adopted to accomplish the pressure-velocity coupling. At the same time, the second order upwind scheme is used for convective term and second order central difference scheme is applied for diffusion term. Furthermore, convergence criterions are set to be less than 10^{-6} for continuity and less than 10^{-9} for energy.

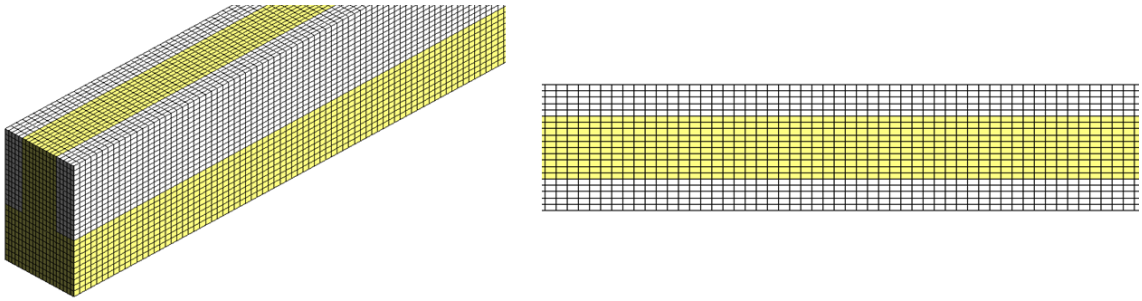

(a) (b)

Fig. 2. Computational grid of CR MCHS (a) Isometric view (b) Top view at x-y plane

Grid independence test is a process to find the optimum mesh structure for CR MCHS which can produce accurate result with the lower time cost. The process is started with the finer mesh structure to the coarser mesh structure. In the grid independence test, the finest mesh of 5.0×10^5 is analysed at Reynolds number of 800. With the same Reynolds number, the number of element is reduced to 1.5×10^5. By considering Nusselt number and pressure drop for each element number, the optimum mesh structure is obtained by calculating the relative error using following equation:

$$e\% = \left| \frac{J_2 - J_1}{J_1} \right| \times 100 \tag{7}$$

Where J_1 represents the value of Nusselt number and pressure drop for the finer mesh structure while J_2 represents the value of Nusselt number and pressure drop for the coarser mesh structure. Based on the relative error presented in Table 3 for each element number, it clearly observed that element number of 3.0×10^5 has a reasonable accuracy compared to the other element numbers and thus can be used in further analysis.

Table 3
Grid independency test

Grid number ($\times10^5$)	Nu	e%	Pressure drop (Pa)	e%
5.0	8.07	-	64599.66	-
4.0	8.07	0%	64574.90	0.038%
3.5	8.07	0%	64557.65	0.065%
3.0	8.07	0%	64535.46	0.099%
2.5	8.07	0%	64507.85	0.142%
2.0	8.07	0%	64480.42	0.185%
1.5	8.07	0%	64465.21	0.200%

3.4 Data Reduction

This section presents the relevant expressions that used to calculate the characteristics of heat transfer and fluid flow in the CR MCHS. Re number, hydraulic diameter and apparent friction factor are expressed in Eq. (8), Eq. (9) and Eq. (10), respectively.

$$\mathrm{Re} = \frac{\rho u_m D_h}{\mu} \tag{8}$$

$$D_h = \frac{2H_c W_c}{H_c + W_c} \tag{9}$$

$$f_{app,ave} = \frac{2D_h \Delta P}{Lt\rho u_m^2} \tag{10}$$

Where D_h, L_t and ΔP are hydraulic diameter, total length of microchannel and pressure drop across microchannel, respectively. Average heat transfer coefficient and the average Nusselt number are given by:

$$h_{ave} = \frac{q_w A_{film}}{A_{con.}(T_{W,ave} - T_{f,ave})} \tag{11}$$

$$Nu_{ave} = \frac{h_{ave} D_h}{k_f} \tag{12}$$

Where q_w, A_{film}, A_{cond}, $T_{w,ave}$ *and* $T_{f,ave}$ are the heat flux per unit area, heated area, convection heat transfer area, average temperature of wall and average temperature of fluid, respectively.

4. Results

In order to verify the accuracy of the simulation model approach, data that obtained from simulation analysis such as the local Nusselt number of CR MCHS is validated with Philips [17] correlation:

$$Nu_X = 1.0958\left[\frac{23.315 + 27038(X) + 1783300(X)^2}{1 + 3049(X) + 472520(X)^2 - 35714(X)^3}\right] \tag{13}$$

$$X = \frac{x}{D_h \,\mathrm{Re}\,\mathrm{Pr}} \tag{14}$$

The validation result has been illustrated in Figure 3. It clearly shows the simulation result has a good agreement with the correlation. This agreement indicates that the simulation model approach can be adopted to predict the fluid flow and heat transfer characteristic in CR MCHS.

Hydrodynamic entrance in laminar flow is very important characteristic that need to be considered in microchannel innovation in order to know whether our analysis is in developing region or developed region. This is because the thermal resistance is higher in the developed region compare to in the developing region. In the developed region, the Nusselt number along the microchannels is quite similar due to the constant velocity profile in the channels. As shown in Figure 4, the Re number affects the hydrodynamic entrance length and thus influence the Nusselt number in CR MCHS. For the lower Re number, the hydrodynamic entrance length is shorter than for the higher Re number. Means that thermal resistance at the lower Re number is higher than in the higher Re number. For the Re number of 100, it obtains the highest thermal resistance due to the short hydrodynamic entrance length of 3 mm from the inlet channel. However, the hydrodynamic entrance length of Re = 800 close to 9 mm which contributes to the higher rate of heat transfer attributed to the less thermal resistance in that region.

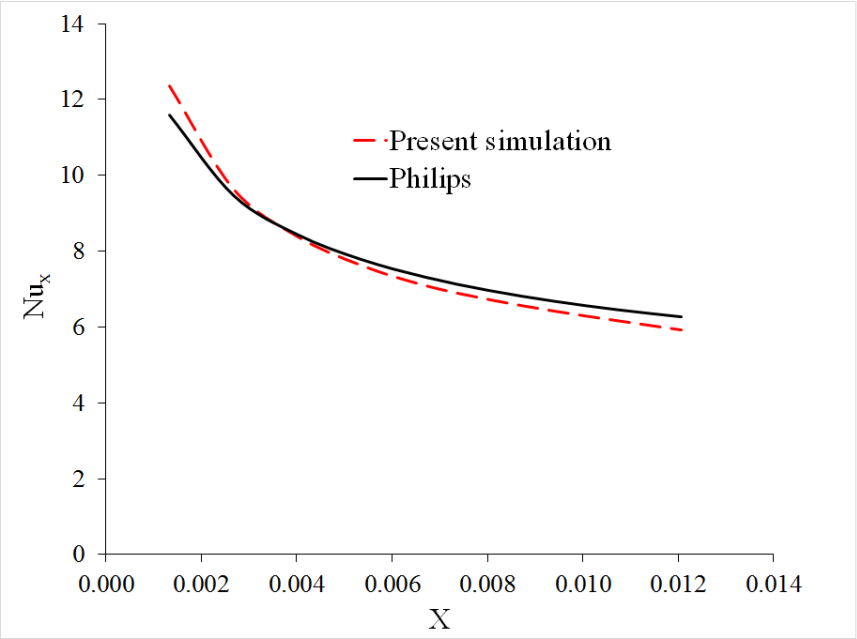

Fig. 3. Model validation (a) Local Nusselt number according to Philips [17]

To analyse the effect of hydrodynamic entrance length on heat transfer performance in CR MCHS, the temperature distribution at the centre hydraulic of CR MCHS is illustrated as shown in Figure 5. At the same location, the Figure 5 shows that CR MCHS at Re number of 800 obtain the superior heat transfer performance than the others due to less thermal resistance in developing region. However, for the Re number of 100, it obtains the lowest thermal performance due to thermal resistance in developed region.

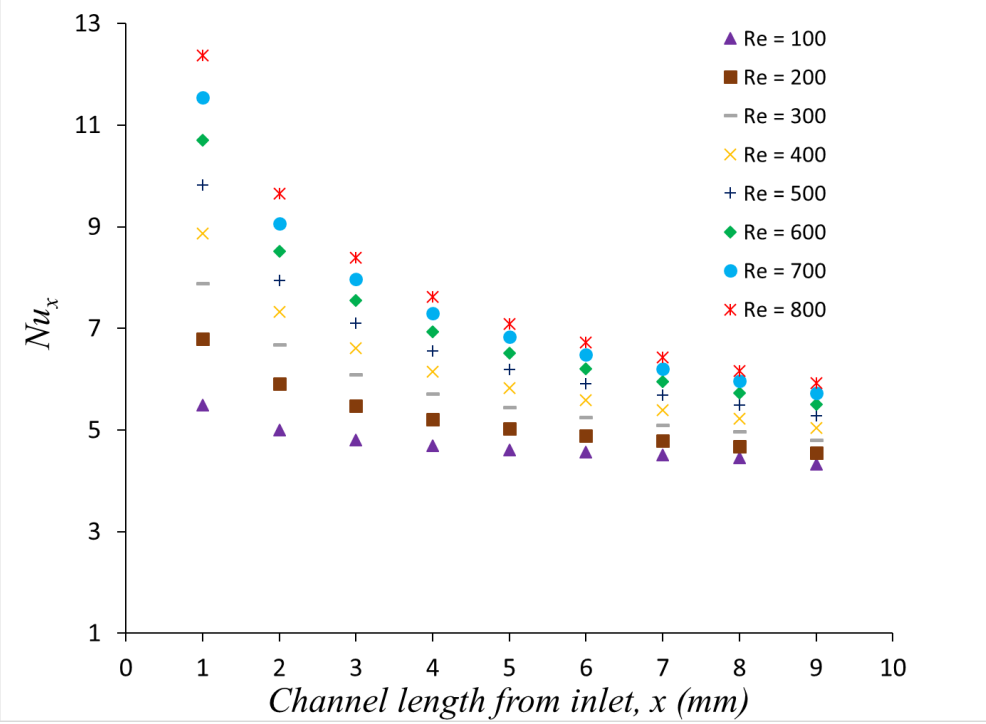

Fig. 4. Local Nusselt number at the channel length

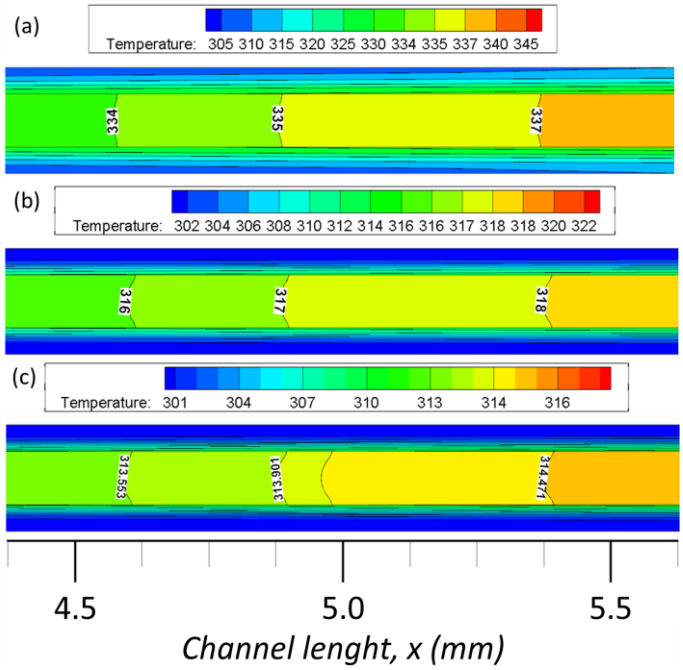

Fig. 5. Temperature distribution (K) in CR MCHS on x-y plane (z = 0.25mm) at (a) Re = 100 (b) 500 (c) 800

Even though the heat transfer performance of the higher Re number shows a superior performance, it also has a drawback on pumping power consumption due to the highest wall shear stress in the hydrodynamic entrance region of CR MCHS. As consequence, the pressure drop is highest in the developing region, which increases the average friction factor for the whole microchannel of CR MCHS and thus increases the pumping power consumption. It can be clearly seen in Figure 6. The Figure 6 illustrates that CR MCHS at Re = 800 obtains the highest pressure distribution compare to the other Re numbers. For the Re number of 100, the flow mostly in the fully developed region whereby the pressure gradient and the shear stress in flow are in balance.

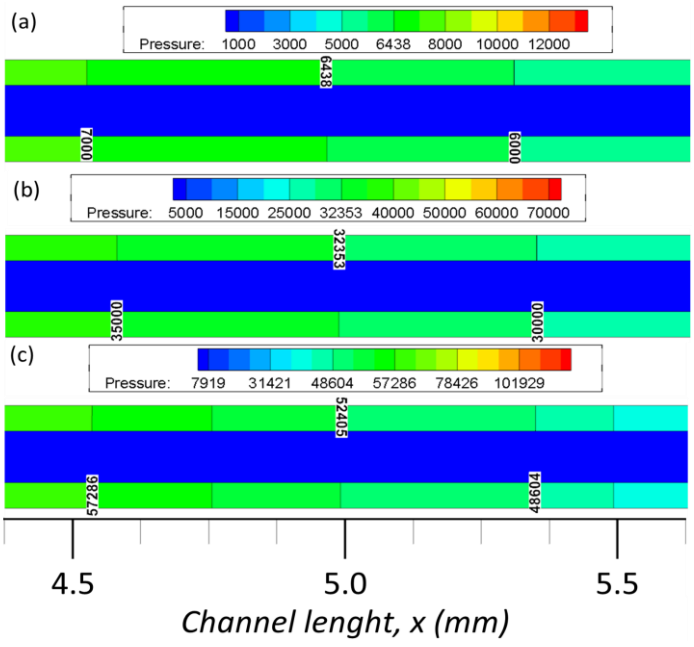

Fig. 6. Pressure distribution (Pa) in CR MCHS on x-y plane (z = 0.25mm) at (a) Re = 100 (b) 500 (c) 800

4. Conclusions

Hydrodynamic entrance length in the straight channel such as rectangular microchannel heat sink is a significant characteristic that need to be considered in microchannel innovation. In this study, the effect of hydrodynamic entrance length on fluid flow and heat transfer characteristic had been studied numerically for the Re number of 100 to 800. The following conclusions can be drawn from the present study:

a) The thermal resistance in the hydrodynamic entrance region of CR MCHS is lower than in the developed region.
b) Pressure drop in the developing region is higher than developed region due to the highest wall shear stress in the entrance region.
c) For hydrodynamic diameter, D_h = 133 μm, the hydrodynamic entrance length of Re = 100 is 3 mm from channel inlet, while Re = 800 is 9 mm from the channel inlet.

Acknowledgement
Authors wish to thanks Universiti Teknologi Malaysia for supporting this research activity under Takasago grant (R.K130000.7343.4B314).

References

[1] Sidik, Nor Azwadi Che, Muhammad Noor Afiq Witri Muhamad, Wan Mohd Arif Aziz Japar, and Zainudin A. Rasid. "An overview of passive techniques for heat transfer augmentation in microchannel heat sink." *International Communications in Heat and Mass Transfer* 88 (2017): 74-83. https://doi.org/10.1016/j.icheatmasstransfer.2017.08.009
[2] Black, James R. "Electromigration—A brief survey and some recent results." *IEEE Transactions on Electron Devices* 16, no. 4 (1969): 338-347. https://doi.org/10.1109/T-ED.1969.16754
[3] Ghani, Ihsan Ali, Nor Azwadi Che Sidik, and Natrah Kamaruzaman. "Hydrothermal performance of microchannel heat sink: The effect of channel design." *International Journal of Heat and Mass Transfer* 107 (2017): 21-44. https://doi.org/10.1016/j.ijheatmasstransfer.2016.11.031
[4] Farsad, E., S. P. Abbasi, M. S. Zabihi, and J. Sabbaghzadeh. "Numerical simulation of heat transfer in a micro channel heat sinks using nanofluids." *Heat and mass transfer* 47, no. 4 (2011): 479-490. https://doi.org/10.1007/s00231-010-0735-y
[5] Qin, Yap Zi, Amer Nordin Darus, and Nor Azwadi Che Sidik. *Numerical analysis on natural convection heat transfer of a heat sink with cylindrical pin fin*. Vol. 695. Trans Tech Publications Ltd, 2015. https://doi.org/10.4028/www.scientific.net/AMM.695.398
[6] Shen S, Xu J, Zhou J, Chen Y. Flow and heat transfer in microchannels with rough wall surface. energy conversion and management. 2006;47(11-12):1311-25. https://doi.org/10.1016/j.enconman.2005.09.001
[7] Hong F, Cheng P. Three dimensional numerical analyses and optimization of offset strip-fin microchannel heat sinks. International Communications in Heat and Mass Transfer. https://doi.org/10.1016/j.icheatmasstransfer.2009.02.015
[8] Sui Y, Teo C, Lee PS, Chew Y, Shu C. Fluid flow and heat transfer in wavy microchannels. International Journal of Heat and Mass Transfer. 2010;53(13-14):2760-72. https://doi.org/10.1016/j.ijheatmasstransfer.2010.02.022
[9] Deng D, Xie Y, Huang Q, Wan W. On the flow boiling enhancement in interconnected reentrant microchannels. International Journal of Heat and Mass Transfer. 2017;108:453-67. https://doi.org/10.1016/j.ijheatmasstransfer.2016.12.030
[10] Lee YJ, Lee PS, Chou SK. Enhanced Thermal Transport in Microchannel Using Oblique Fins. Journal of Heat Transfer. 2012;134(10). https://doi.org/10.1115/1.4006843
[11] Go JS. Design of a microfin array heat sink using flow-induced vibration to enhance the heat transfer in the laminar flow regime. Sensors and Actuators A: physical. 2003;105(2):201-10.

https://doi.org/10.1016/S0924-4247(03)00101-8
[12] Yeom T, Simon TW, Huang L, North MT, Cui T. Piezoelectric translational agitation for enhancing forced-convection channel-flow heat transfer. International journal of heat and mass transfer. 2012;55(25-26):7398-409. https://doi.org/10.1016/j.ijheatmasstransfer.2012.07.019
[13] Krishnaveni T, Renganathan T, Picardo J, Pushpavanam S. Numerical study of enhanced mixing in pressure-driven flows in microchannels using a spatially periodic electric field. Physical Review E. 2017;96(3):033117. https://doi.org/10.1103/PhysRevE.96.033117
[14] Hessami M-A, Berryman A, Bandopdhayay P, editors. Heat Transfer Enhancement in an Electrically Heated Horizontal Pipe Due to Flow Pulsation. ASME 2003 International Mechanical Engineering Congress and Exposition; 2003.
[15] Zhang H, Li S, Cheng J, Zheng Z, Li X, Li F. Numerical study on the pulsating effect on heat transfer performance of pseudo-plastic fluid flow in a manifold microchannel heat sink. Applied Thermal Engineering. 2018;129:1092-105. https://doi.org/10.1016/j.applthermaleng.2017.10.124
[16] Service, Robert F. "Coming soon: the pocket DNA sequencer." *Science (New York, NY)* 282, no. 5388 (1998): 399. https://doi.org/10.1126/science.282.5388.399
[17] Phillips, Richard J. "Microchannel heat sinks." *Advances in Thermal Modeling of Electronic Components* (1990).